Geological Survey
of Canada

CURRENT RESEARCH
2002-E13

Fluid compositions and temperature-pressure conditions of intrusion-related gold systems in southwestern New Brunswick — a fluid-inclusion study

G. Chi

2002

Natural Resources Canada
Ressources naturelles Canada

Canada

©Her Majesty the Queen in Right of Canada 2002
ISSN 1701-4387
Catalogue No. M44-2002/E13E
ISBN 0-660-18855-4

Available in Canada from the
Geological Survey of Canada Bookstore website at:
http://www.nrcan.gc.ca/gsc/bookstore (Toll-free: 1-888-252-4301)

A copy of this publication is also available for reference by depository libraries across Canada through access to the Depository Services Program's website at http://dsp-psd.pwgsc.gc.ca

Price subject to change without notice

All requests for permission to reproduce this work, in whole or in part, for purposes of commercial use, resale, or redistribution shall be addressed to: Earth Sciences Sector Information Division, Room 402, 601 Booth Street, Ottawa, Ontario K1A 0E8.

Author's address

G. Chi (guoxiang.chi@uregina.ca)
Department of Geology
University of Regina
Regina, Saskatchewan S4S 0A2

Publication approved by GSC Quebec

103-04442/

Fluid compositions and temperature-pressure conditions of intrusion-related gold systems in southwestern New Brunswick — a fluid-inclusion study[1]

G. Chi

Chi, G., 2002: Fluid compositions and temperature-pressure conditions of intrusion-related gold systems in southwestern New Brunswick — a fluid-inclusion study; Geological Survey of Canada, Current Research 2002-E13, 11 p.

Abstract: Several gold occurrences discovered in the granite-dominated districts of southwestern New Brunswick share some similarities with a newly recognized type of intrusion-related gold systems. This paper presents fluid inclusion microthermometry data from four gold occurrences in southwestern New Brunswick (Poplar Mountain, Clarence Stream, Jimmy Hill, and Kedron). These data suggest that mineralizing fluid systems for Poplar Mountain, Clarence Stream, and Jimmy Hill may be approximated by H_2O-NaCl-CO_2-CH_4 (characteristic of the deeper part of the new type of intrusion-related gold systems) and those for Kedron, by H_2O-NaCl with high salinities (characteristic of the shallower part of the systems). Fluid temperatures are mainly 220°C to 280°C for Poplar Mountain, 180°C to 280°C for Clarence Stream, 230°C to 330°C for Jimmy Hill, and 120°C to 200°C for Kedron. Fluid pressures are probably 785 to 1364 bars for Poplar Mountain, 594 to 1226 bars for Clarence Stream, and 965 to 1764 bars for Jimmy Hill.

Résumé : Plusieurs indices aurifères découverts dans les districts principalement granitiques du sud-ouest du Nouveau-Brunswick s'apparentent à un type nouvellement reconnu de systèmes aurifères associés à des intrusions. Cet article présente des données microthermométriques d'inclusions fluides provenant de quatre indices aurifères dans le sud-ouest du Nouveau-Brunswick (Poplar Mountain, Clarence Stream, Jimmy Hill et Kedron). Ces données suggèrent que les fluides minéralisateurs des indices de Poplar Mountain, de Clarence Stream et de Jimmy Hill seraient composés de H_2O-NaCl-CO_2-CH_4 (composition caractéristique de la partie la plus profonde du type nouvellement reconnu de systèmes aurifères associés à des intrusions) et que les fluides minéralisateurs de l'indice de Kedron seraient constitués de H_2O-NaCl et présenteraient de fortes teneurs en sel (ce qui est caractéristique de la partie moins profonde des systèmes). En général, les températures des fluides de Poplar Mountain varient entre 220 °C et 280 °C, celles de Clarence Stream, entre 180 °C et 280 °C, celles de Jimmy Hill, entre 230 °C et 330 °C et celles de Kedron, entre 120 °C et 200 °C. Les pressions des fluides de Poplar Mountain se situeraient entre 785 et 1 364 bars, celles de Clarence Stream, entre 594 et 1 226 bars, et celles de Jimmy Hill, entre 965 et 1 764 bars.

[1] Contribution to Targeted Geoscience Initiative

INTRODUCTION

A number of gold occurrences have recently been discovered in the granite-dominated districts of southwestern New Brunswick (McLeod and McCutcheon, 2000; McLeod, 2002), which is best known for its W-Sn-Mo-Sb resources. Gold mineralization occurs from within granitic intrusions, through contact zones, to country rocks relatively far away from the intrusions. These new discoveries in southwestern New Brunswick coincide with the worldwide recognition of an economically important new type of gold deposits related to granitic intrusions in magmatic provinces formerly known for W and/or Sn deposits (Thompson et al., 1999; Lang et al., 2000; Lang and Baker, 2001). The gold mineralizations in southwestern New Brunswick shares some similarities with the newly recognized type of intrusion-related gold systems (D. Hoy, unpub. rept., 2000; Chi et al., 2002; McLeod, 2002), and their genetic link with granite intrusions constitutes the subject of an ongoing Geological Survey of Canada Targeted Geoscience Initiative (TGI) project.

The newly recognized type of intrusion-related gold systems differs from porphyry base metal-gold systems in many ways, including tectonic setting, intrusion geochemistry, element association, style of mineralization and alteration, and fluid composition (Thompson et al., 1999; Lang et al., 2000; Lang and Baker, 2001). The deeper part of the newly recognized type of intrusion-related gold systems commonly contains carbonic fluid inclusions whereas porphyry base metal-gold systems are characterized by high-salinity, halite-bearing fluid inclusions (Lang et al., 2000). Thus, fluid composition is an important aspect to be considered in gold metallogenic models in southwestern New Brunswick. In addition, fluid temperature and pressure provide key constraints on the conditions of formation of the gold deposits. The object of this study is to characterize the compositional systems of the fluids related to gold mineralization as well as temperature and pressure conditions, through fluid-inclusion microthermometry studies of selected gold occurrences in southwestern New Brunswick.

REGIONAL AND LOCAL GEOLOGY

The northern Appalachian Orogen is divided into several northeast-trending Lower Paleozoic tectonic zones, which are overlain by Middle Paleozoic basins and then by Upper Paleozoic successor basins (Williams, 1995). In New Brunswick, the Lower Paleozoic tectonic zones include, from northwest to southeast, the Dunnage, Gander, and Avalon zones (Fig. 1). The Dunnage and Gander zones collided when the Iapetus Ocean closed in the Late Ordovician to Late Silurian (van Staal, 1994). The Avalon Zone was amalgamated to the Gander Zone by accretion of the Ellsworth Arc in the Early Ordovician and of the Caledonia Terrane in the Late Silurian (Fyffe et al., 1999). The Gander Zone is overlain by the Late Ordovician to Early Devonian Matapedia and Fredricton basins, and the Avalon Zone, by the Late Silurian Mascarene Basin; all are overlain by the Late Devonian to Early Permian Maritimes Basin (Fig. 1).

Two major granitoid batholiths occur in southwestern New Brunswick. The Pokiok Batholith intruded Cambrian to Middle Ordovician strata of the Miramichi Terrane of the Gander Zone and Late Silurian strata of the Fredricton Basin (Fig. 1). Isotopic ages for the batholith range from 415 to 402 Ma (*see* McLeod et al., 1994). The St. George Batholith intruded Precambrian strata of the Caledonia Terrane, Ordovician strata of the St. Croix Terrane of the Gander Zone, and Late Silurian strata of the Mascarene Basin (Fig. 1). It is composed of five intrusive suites ranging in age from 430 to 360 Ma (*see* McLeod et al., 1994). Although the batholiths are located near the Gander–Dunnage and Gander–Avalon terrane boundaries, their emplacement took place after amalgamation of the terranes and therefore is not directly related to plate subduction processes.

A number of gold occurrences are found around these granitoid batholiths, the more important being Poplar Mountain (north of the Pokiok Batholith), Lake George (southeast contact zone of the Pokiok Batholith), and Jimmy Hill and Clarence Stream (contact zone of the Magaguadavic phase of the St. George Batholith) (Fig. 1). Gold mineralization (e.g. Kedron) is also found associated with small granite intrusions of the Pomeroy Suite of the St. George Batholith, occurring as satellite intrusions north of the batholith. Fluid-inclusion studies have been carried out for the Lake George Sb-W-Mo deposit (Seal et al., 1987), which was later found to contain ore-grade gold mineralization (Morrissy, 1991). This paper presents the first fluid-inclusion study results for the Poplar Mountain, Clarence Stream, Jimmy Hill, and Kedron gold occurrences.

Poplar Mountain gold occurrence

The Poplar Mountain gold occurrence is hosted in the Poplar Mountain Volcanic Complex, a subvolcanic and volcanic complex of unknown age located about 8 km north of the Pokiok granite batholith (411–402 Ma) and close to the regional Woodstock Fault, which separates the Cambrian–Middle Ordovician strata of the Miramichi Terrane (Gander Zone) from the Late Ordovician–Early Devonian Matapedia Basin to the northwest (Fig. 1). The Poplar Mountain Volcanic Complex is composed of porphyritic dacite, dacitic volcaniclastic rocks, and basaltic volcanic rocks. The porphyritic dacite in the centre of the complex is interpreted to be a subvolcanic intrusion surrounded by contemporaneous dacitic volcaniclastic rocks, and predates the basalt (Chi and Watters, 2002). The mineralization comprises several zones that are hosted mainly by the porphyritic dacite and to a lesser extent by basalt and dacitic volcaniclastic rocks. The mineralized zones range from a few metres up to 60 m in width, and gold assay values range from 0.26 to 5.53 g/t (Freewest Resources Canada Inc., unpub. rept., 1999). The mineralized zones are characterized by multidirectional fractures and quartz-carbonate-sericite alteration. Gold is associated with arsenopyrite, which is disseminated in the volcanic and subvolcanic rocks, and occurs in quartz-carbonate-sericite veins and stockworks, as well as in the breccia matrix. The host rocks have been extensively altered by

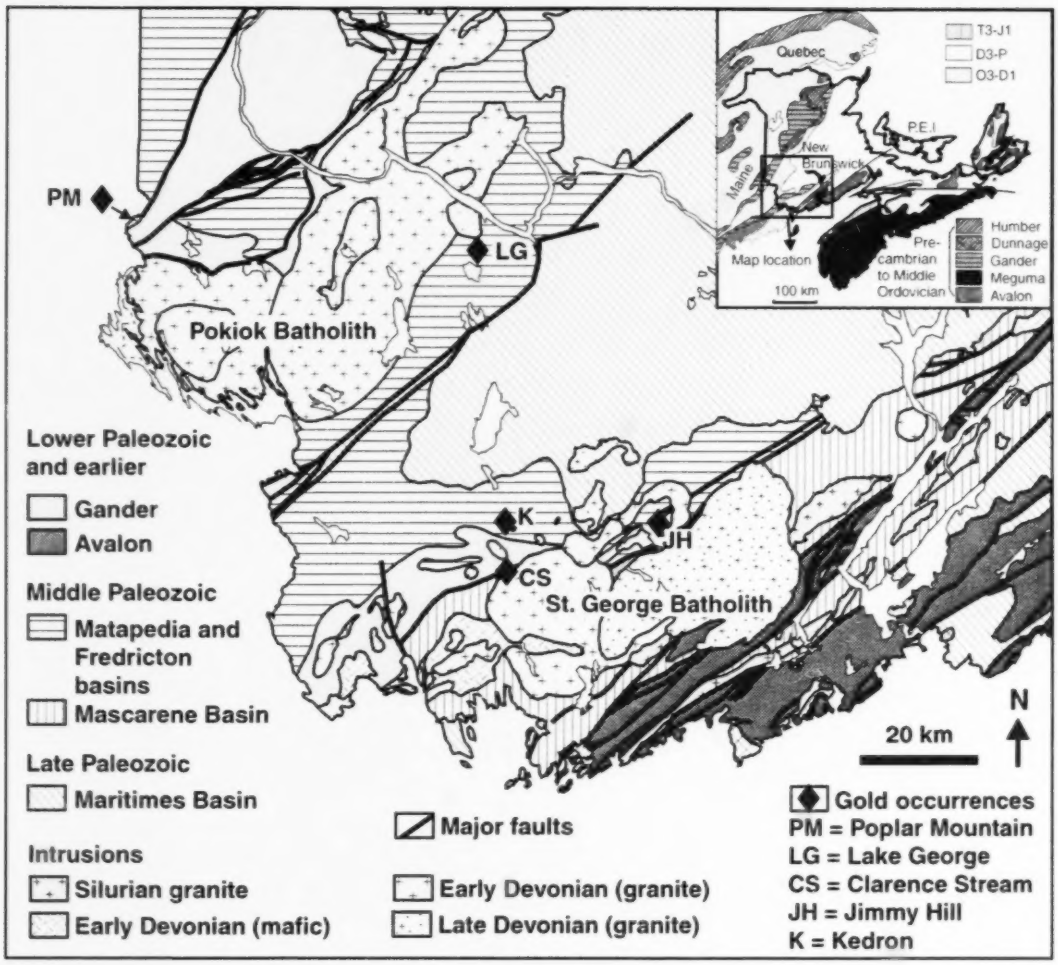

Figure 1. *Regional geological map of southwestern New Brunswick* (modified from *New Brunswick Department of Natural Resources and Energy, 2000*), *showing the location of the gold occurrences discussed in this paper.*

chlorite±illite±carbonate, over which is superimposed quartz-sericite-carbonate alteration. The latter is closely related to mineralization (Chi and Watters, 2002).

Clarence Stream gold occurrence

The Clarence Stream gold occurrence is located in the contact zone between the Magaguadavic granite (396 Ma) of the St. George batholith (418–367 Ma) and Late Silurian clastic sedimentary rocks of the Mascarene Basin, close to the Gander–Avalon terrane boundary (Fig. 1). Mineralization is hosted in shear zones developed in hornfels and metagabbro (Thorne et al., 2001). The mineralized zones, about 2 km along strike, are parallel to the contact zone and the strata, which trend northeast and dip northwest. Diamond-drilling programs carried out by Freewest Resources Canada Inc. revealed several relatively high-grade intersections, including 15.06 g/t Au over 21 m in the East Zone, and 6.64, 7.21, 7.8, and 21.51 g/t gold over widths of 12.5, 12, 14.9, and 9.5 m, respectively, in the Central Zone (Robertson, 2001). The shortest distance between the mineralization zones and the Magaguadavic granite intrusion is less than 200 m. Visible and invisible gold are associated with arsenopyrite, pyrrhotite, and stibnite, which are disseminated in host rocks and occur in quartz veins and locally in pegmatite veins (Thorne et al., 2001). The mineralization is associated with silicification and sericitization, which are postdated by epidote alteration. Quartz and pegmatite veins locally show extensional features such as angular fragments of wall rock within the veins, but they are commonly boudinaged and transposed parallel to the shear zones as a result of postmineralization deformation.

Jimmy Hill gold occurrence

The Jimmy Hill gold occurrence is located in the contact zone between the Magaguadavic granite and hornfelsed Ordovician wacke of the Gander Zone (Fig. 1). Mineralization occurs as quartz veins up to 25 cm wide and stockworks with random orientations. Visible gold occurs in the veins

along with wolframite, bismuthinite, arsenopyrite, molybdenite, pyrite, chalcopyrite, galena, and sphalerite. One grab sample yielded a gold value of 5.9 g/t, and two drill cores ran gold values of 3.6 and 9.48 g/t over 0.2 and 0.7 m, respectively (New Brunswick Mineral Occurrence Database). Muscovite and tourmaline occur in some veins. The mineralized veins are located about 400 m from the contact zone with the Magaguadavic granite, and a sulfide-rich pegmatite pod is found within the granite (New Brunswick Mineral Occurrence Database).

Kedron gold occurrence

The Kedron gold occurrence is located in the contact zone between the Kedron granite stock and hornfelsed sandstone and siltstone of the Late Silurian Kingsclear Group of the Fredricton Basin (Fig. 1). The Kedron granite stock is probably similar to those related to the Mount Pleasant W-Sn-Mo mineralization, which have an isotopic age of about 360 Ma (*see* McLeod et al., 1994). According to the New Brunswick Mineral Occurrence Database, mineralization at Kedron occurs as disseminations, quartz veins, and stockworks in the hornfels and granite, which are chloritized and greisenized. Metallic minerals include wolframite, pyrite, molybdenite, sphalerite, chalcopyrite, cassiterite, arsenopyrite, galena, and pyrrhotite. Gangue minerals include quartz, fluorite, tourmaline, and calcite. An anomalous gold value (0.2 ppm) was found in one grab sample (New Brunswick Mineral Occurrence Database).

METHOD

Fluid inclusions are studied in quartz and sphalerite that are paragenetically related to gold mineralization. No definite relationship between fluid inclusion entrapment and crystal growth can be established in any of the samples from the four occurrences. Thus, fluid inclusions occurring in clusters, in isolation, and randomly are interpreted to represent fluids trapped during gold mineralization. In all the occurrences, fluid immiscibility is indicated by the coexistence of vapour- and liquid-rich fluid inclusions. Heterogeneous trapping is commonly indicated by varied vapour/liquid ratios. However,

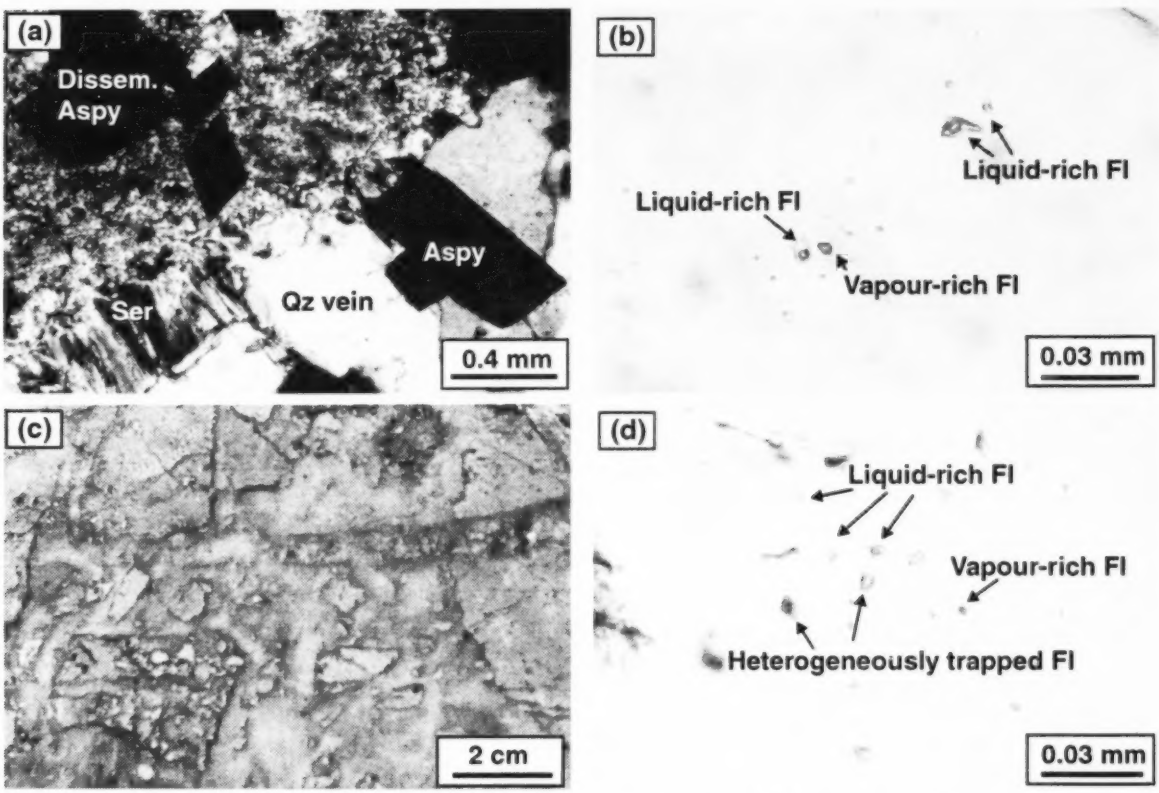

Figure 2. *Petrography of fluid inclusions and host minerals from the Poplar Mountain gold occurrence.* ***a****) Gold-bearing arsenopyrite (Aspy) disseminated in porphyritic dacite and coprecipitated with quartz and sercite (Ser) in a vein (97SW-46).* ***b****) Coexistence of liquid-rich and vapour-rich fluid inclusions in clusters in quartz; note consistent vapour/total ratios of the liquid-rich inclusions (97SW-46).* ***c****) Dacite fragments cemented by quartz; arsenopyrite occurs in both the fragments and the matrix (GC01-123).* ***d****) Coexistence of liquid-rich, vapour-rich, and heterogeneously trapped fluid inclusions in quartz; note consistent vapour/total ratios of the liquid-rich inclusions (GC01-123).*

homogeneously trapped fluid inclusions are commonly present and in some cases abundant, and their relatively consistent homogenization temperatures (within individual fluid-inclusion assemblages) are interpreted to reflect the trapping temperatures. Heterogeneously trapped fluid inclusions (i.e. those with varied V/L ratios within individual fluid-inclusion assemblages) were not studied. The homogenization temperatures of vapour-rich inclusions were rarely measurable. Carbonic fluid inclusions with no visible aqueous phase were treated as pure CO_2 inclusions for isochoric calculation. Isochoric calculations for liquid-rich inclusions show highly varied pressure values that strongly depend on the equation of state chosen, and therefore were not used. Fluid-inclusion microthermometry was carried out with a USGS-style heating-freezing stage made by Fluid Inc. The precision of temperature measurements is ±0.2°C at low temperatures and ±1°C at high temperatures. Isochoric calculations were made by using the Brown-Lamb equation in the Flincor program of Brown (1989).

MICROTHERMOMETRY RESULTS

Poplar Mountain

Four samples were selected for fluid inclusion study. Three (GC01-69, GC01-63, 97SW-46) are quartz veins associated with arsenopyrite and sericite (Fig. 2a); the fourth (GC01-123) is quartz associated with arsenopyrite in the matrix of a dacite breccia (Fig. 2c). Gold concentrations are 1.04 ppm (GC01-69), 1.53 ppm (GC01-63), >5.0 ppm (GC01-123), and 3.45 ppm (97SW-46).

Three types of fluid inclusions are found: liquid-rich (vapour/total ratio ≤30%), vapour-rich (vapour/total ratio near 100%, i.e. liquid phase invisible), and those with varied vapour/total ratios (Fig. 2b, d). The coexistence of these types of fluid inclusions strongly suggests that two immiscible fluid phases were present during mineralization, i.e. a vapour phase and a liquid phase. The third type of fluid inclusion resulted from heterogeneous trapping of the two phases at varied proportions. Table 1 provides microthermometry results for individual fluid-inclusion assemblages.

Most liquid-rich fluid inclusions contain CO_2, which is indicated by the melting temperatures of CO_2 and clathrate. Melting temperatures of CO_2 range from -57.2°C to -56.6°C, ice melting temperatures, from -5.6°C to -1.8°C, gas hydrate melting temperatures, from +5.8°C to +8.8°C, homogenization temperatures of CO_2, from +25.1°C (to liquid) to +29.2°C (to vapour), and final homogenization temperatures, mainly from 220°C to 280°C (Table 1; Fig. 3). Fluid salinities calculated from gas hydrate melting temperatures range from

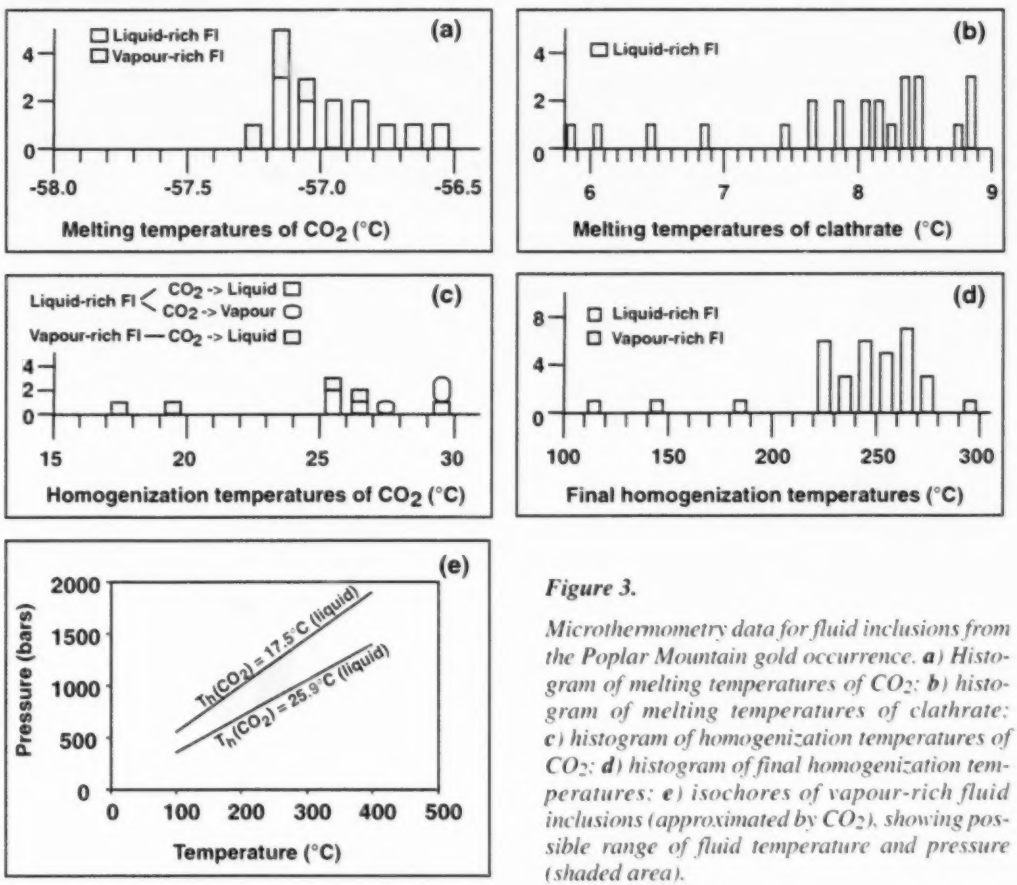

Figure 3.

*Microthermometry data for fluid inclusions from the Poplar Mountain gold occurrence. **a**) Histogram of melting temperatures of CO_2; **b**) histogram of melting temperatures of clathrate; **c**) histogram of homogenization temperatures of CO_2; **d**) histogram of final homogenization temperatures; **e**) isochores of vapour-rich fluid inclusions (approximated by CO_2), showing possible range of fluid temperature and pressure (shaded area).*

Table 1. Fluid-inclusion microthermometry data.

Sample	Host mineral	Occurrence	Size (μ m)	V/T %	$T_{m\text{-}CO_2}$ (°C) Range	$T_{m\text{-}CO_2}$ (°C) Mean (n)	$T_{m\text{-}ice}$ (°C) Range	$T_{m\text{-}ice}$ (°C) Mean (n)	$T_{m\text{-}clath}$ (°C) Range	$T_{m\text{-}clath}$ (°C) Mean (n)	$T_{h\text{-}CO_2}$ (°C) Range	$T_{h\text{-}CO_2}$ (°C) Mean (n)	Salinity (wt.% NaCl equiv.) Range	Salinity (wt.% NaCl equiv.) Mean (n)	T_h (°C) Range	T_h (°C) Mean (n)
Poplar Mountain occurrence																
GC01-69	Quartz	Cluster	6 ~ 7	20	-56.8	-57.1 (1)	-2.8	-2.8 (1)	8.8 ~ 8.8	8.8 (2)	-	-	-	-	261.0 ~ 274.2	267.6 (2)
	(assoc. with	Isolated	7	20	-	-	-	-	-	-	-	-	-	-	257.4	257.4 (1)
	arsenopyrite)	Isolated	8	25	-57.2	-57.2 (1)	-	-	8.8	8.8 (1)	25.1 L	25.1 (1)	2.4	2.4 (1)	265.7	265.7 (1)
		Random	6 ~ 12	20	-56.9 ~ -57.0	-57.0 (2)	-3.4	-3.4 (1)	8.5 ~ 8.9	8.8 (4)	29.8 ~ 29.8 V	29.8 (2)	2.2 ~ 3.0	2.6 (2)	239.2 ~ 266.0	251.1 (4)
		Random	7 ~ 11	20	-56.6	-56.6 (1)	-3.4	-3.4 (1)	7.7 ~ 8.7	8.2 (2)	29.4 ~ 30.0 V	29.7 (2)	2.6 ~ 4.5	3.6 (2)	230.9 ~ 240.5	234.6 (3)
		Random	10 ~ 14	15	-56.7 ~ -56.8	-56.7 (2)	-2.8	-2.8 (1)	8.1 ~ 8.7	8.4 (2)	29.0 ~ 29.4 L	29.2 (2)	2.6 ~ 3.8	3.3 (2)	202.8 ~ 241.5	221.2 (3)
GC01-123	Quartz	Isolated	10	15	-56.8	-56.8 (1)	-5.0	-5.0 (1)	8.1	8.1 (1)	-	-	-	-	242.0	242.0 (1)
	(cement	Isolated	7	15	-	-	-3.4	-3.4 (1)	8.4	8.4 (1)	-	-	-	-	220.3	220.3 (1)
	in	Isolated	7	15	-	-	-3.5	-3.5 (1)	8.7	8.7 (1)	-	-	-	-	248.8	248.8 (1)
	breccia,	Isolated	8	15	-	-	-	-	-	-	-	-	-	-	221.9	221.9 (1)
	assoc.	Isolated	8	15	-	-	-	-	-	-	-	-	-	-	231.3	231.3 (1)
	with	Scattered	9 ~ 9	10	-	-	-1.7 ~ -2.3	-2.0 (2)	-	-	-	-	2.9 ~ 3.9	3.4 (2)	138.5 ~ 156.5	147.5 (2)
	arsenopyrite)	Scattered	12	20	-57.2	-57.2 (1)	-5.1	-5.1 (1)	8.0	8.0 (1)	25.5 L	25.5 (1)	4.0	4.0 (1)	262.8	262.8 (1)
		Cluster	5 ~ 9	15	-	-	-4.7	-4.7 (1)	7.4	7.4 (1)	-	-	-	-	216.9 ~ 241.8	229.4 (2)
		Isolated	10	10	-56.9	-56.9 (1)	-5.1	-5.1 (1)	7.6	7.6 (1)	-	-	-	-	247.4	247.4 (1)
		Isolated	10	10	-57.0	-57.0 (1)	-5.2	-5.2 (1)	7.8	7.8 (1)	-	-	-	-	238.0	238.0 (1)
		Isolated	12	25	-56.9	-56.9 (1)	-	-	6.0	6.0 (1)	-	-	-	-	252.1	252.1 (1)
		Cluster	10 ~ 11	25	-57.0 ~ -57.1	-57.1 (2)	-4.2	-4.2 (1)	5.8	5.8 (1)	27.8 ~ 28.0 V	27.9 (2)	7.8	7.8 (1)	268.5 ~ 270.8	269.7 (2)
		Cluster	9	15	-	-	-5.2	-5.2 (1)	6.8	6.8 (1)	-	-	-	-	187.7	187.1 (1)
		Cluster	4 ~ 8	100	-57.3 ~ -57.3	-57.3 (2)	-	-	-	-	14.9 ~ 20.1 L	17.5 (4)	-	-	-	-
		Random	4 ~ 8	100	-57.2 ~ -57.2	-57.2 (2)	-	-	-	-	18.5 ~ 20.9 L	19.2 (5)	-	-	-	-
			7 ~ 10	15	-	-	-5.3	-5.3 (1)	6.4	6.4 (1)	-	-	-	-	239.6 ~ 242.7	241.2 (2)
GC01-63	Quartz	Random	5 ~ 7	10	-	-	-1.6 ~ -1.9	-1.8 (2)	-	-	-	-	2.7 ~ 3.2	3.0 (2)	108.2 ~ 119.1	113.2 (4)
	(assoc. with	Random	6 ~ 9	30	-56.9 ~ -57.4	-57.2 (7)	-3.5	-3.5 (1)	6.9 ~ 8.4	7.6 (5)	26.0 ~ 27.0 L	26.5 (7)	3.2 ~ 5.9	4.7 (5)	247.2 ~ 287.2	262.9 (7)
	arsenopyrite)	Cluster	6 ~ 7	25	-	-	-5.4	-5.4 (1)	8.2 ~ 8.4	8.3 (2)	-	-	-	-	264.2 ~ 269.2	266.7 (2)
		Isolated	7	25	-	-	-	-	8.4	8.4 (1)	-	-	-	-	250.7	250.7 (1)
97SW-46	Quartz	Cluster	6 ~ 7	15	-	-	-5.5 ~ -5.7	-5.6 (2)	7.8	7.8 (1)	-	-	-	-	212.6 ~ 227.8	220.2 (2)
	(assoc. with	Isolated	5	20	-	-	-5.5	-5.5 (1)	8.1	8.1 (1)	-	-	-	-	277.2	277.2 (1)
	arsenopyrite)	Isolated	4	15	-	-	-	-	-	-	-	-	-	-	267.3	267.3 (1)
		Isolated	4	15	-	-	-	-	-	-	-	-	-	-	220.2	220.2 (1)
		Cluster	6	20	-	-	-	-	8.0	8.0 (1)	-	-	-	-	279.3	279.3 (1)
			7	85	-57.2	-57.2 (1)	-	-	-	-	26.1 L	26.1 (1)	-	-	292.8 V	292.8 (1)
		Isolated	6	20	-	-	-	-	8.3	8.3 (1)	-	-	-	-	246.3	246.3 (1)
		Isolated	9	10	-	-	-	-	-	-	-	-	-	-	252.7	252.7 (1)
		Isolated	6	25	-	-	-	-	-	-	-	-	-	-	273.2	273.2 (1)
		Cluster	5	100	-57.1	-57.1 (1)	-	-	-	-	25.9 L	25.9 (1)	-	-	-	-
			6	20	-	-	-	-	8.3	8.3 (1)	-	-	-	-	244.2	244.2 (1)
Clarence Stream occurrence																
GC01-141	Quartz	Cluster	7 ~ 10	15	-	-	-3.8	-3.8 (1)	-	-	-	-	6.1	6.1 (1)	269.1 ~ 288.3	279.0 (4)
	(assoc. with	Scattered	8 ~ 15	10	-	-	-9.6 ~ -10.1	-9.9 (3)	-	-	-	-	13.6 ~ 14.1	13.9 (3)	173.8 ~ 220.9	204.7 (6)
	pegmatite)	Isolated	9	10	-	-	-10.5	-10.5 (1)	23.4	23.4 (1)	-	-	-	-	167.8	167.8 (1)
		Isolated	8	10	-	-	-10.3	-10.3 (1)	-	-	-	-	-	-	127.5	127.5 (1)
		Isolated	9	10	-	-	-12.9	-12.9 (1)	25.4	25.4 (1)	-	-	-	-	191.5	191.5 (1)
		Cluster	6	15	-	-	-9.6	-9.6 (1)	29.7	29.7 (1)	-	-	-	-	260.3	260.3 (1)
		Isolated	8	15	-	-	-	-	-	-	-	-	-	-	271.9	271.9 (1)
		Cluster	7 ~ 10	10	-	-	-5.7 ~ -8.7	-7.2 (2)	-	-	-	-	8.8 ~ 12.6	10.7 (2)	174.8 ~ 177.1	175.9 (2)
		Isolated	16	8	-	-	-0.2	-0.2 (1)	-	-	-	-	0.4	0.4 (1)	172.5	172.5 (1)
		Cluster	7 ~ 8	10	-	-	-5.9	-5.9 (1)	-	-	-	-	9.1	9.1 (1)	189.8 ~ 203.8	196.8 (2)
		Isolated	13	8	-	-	-9.1	-9.1 (1)	-	-	-	-	13.0	13.0 (1)	189.5	189.5 (1)
		Cluster	7 ~ 8	10	-	-	-6.2 ~ -6.2	-6.2 (2)	-	-	-	-	9.5 ~ 9.5	9.5 (2)	198.9 ~ 225.4	212.2 (2)
		Fracture	7 ~ 13	10	-	-	-8.8 ~ -9.3	-9.1 (2)	-	-	-	-	12.7 ~ 13.2	13.0 (2)	181.0 ~ 244.3	210.9 (4)
		Fracture	7 ~ 15	10	-	-	-5.2	-5.2 (1)	-	-	-	-	8.1	8.1 (1)	177.7 ~ 202.5	190.9 (4)
		Cluster	9	100	-58.7	-58.7 (1)	-	-	-	-	16.6 V	16.6 (1)	-	-	-	-
			6 ~ 10	10	-	-	-9.9	-9.9 (1)	-	-	-	-	13.9	13.9 (1)	181.8 ~ 184.3	183.1 (2)
		Cluster	4 ~ 5	10	-	-	-	-	-	-	-	-	-	-	183.3 ~ 195.7	188.8 (3)
		Cluster	6 ~ 8	15	-	-	-7.8	-7.8 (1)	-	-	-	-	11.5	11.5 (1)	203.3 ~ 234.4	218.4 (3)

$T_{m\text{-}clath}$ = melting temperature of clathrate
$T_{m\text{-}ice}$ = ice melting temperature
$T_{m\text{-}CO_2}$ = melting temperature of CO_2

$T_{h\text{-}CO_2}$ = homogenization temperature of CO_2
Th = homogenization temperature
V/T = vapour/total ratio

Table 1 (cont.)

Sample	Host mineral	Occurrence	Size (μ m)	V/T %	$T_{m\text{-}CO_2}$ (°C)		$T_{m\text{-}ice}$ (°C)		$T_{m\text{-}clath}$ (°C)		$T_{h\text{-}CO_2}$ (°C)		Salinity (wt.% NaCl equiv.)		T_h (°C)	
					Range	Mean (n)	Range	Mean (n)	Range	Mean (n)	Range	Mean (n)	Range	Mean (n)	Range	Mean (n)
Clarence Stream occurrence																
GC01-150	Quartz (assoc. with pegmatite)	Scattered	8 ~ 15	12	-	-	-6.3 ~ 9.4	-7.3 (4)	-	-	-	-	9.6 ~ 13.3	10.8 (4)	227.3 ~ 264.0	241.6 (4)
		Isolated	6	30	-	-	-3.7	-3.7 (1)	-	-	-	-	6.0	6.0 (1)	276.8	276.8 (1)
		Isolated	5	30	-	-	-3.7	-3.7 (1)	-	-	-	-	6.0	6.0 (1)	201.2	201.2 (1)
		Scattered	11 ~ 12	12	-	-	-1.8 ~ -3.7	-2.7 (3)	7.4	7.4 (1)	-	-	-	-	192.7 ~ 201.4	197.8 (3)
		Cluster	9 ~ 15	100	-57.5 ~ -57.6	-57.6 (3)	-	-	-	-	19.3 ~ 22.0 L	20.8 (3)	-	-	-	-
		Cluster	6 ~ 8	10	-	-	-3.4	-3.4 (1)	7.0	7.0 (1)	-	-	-	-	202.8 ~ 207.9	205.4 (2)
		Cluster	5 ~ 9	15	-	-	-3.4	-3.4 (1)	7.9	7.9 (1)	-	-	-	-	259.6 ~ 290.6	275.1 (2)
		Cluster	12	10	-	-	-7.7	-7.7 (1)	-	-	-	-	11.4	11.4 (1)	229.9	229.9 (1)
		Cluster	7 ~ 8	10	-	-	-	-	-	-	-	-	11.4	11.4 (1)	187.6 ~ 191.9	189.8 (2)
		Isolated	10	8	-	-	-7.3	-7.3 (1)	-	-	-	-	10.9	10.9 (1)	217.0	217.0 (1)
		Fracture	9	10	-	-	-1.2	-1.2 (1)	-	-	-	-	2.1	2.1 (1)	175.2	175.2 (1)
			5 ~ 15	100	-57.3 ~ -57.4	-57.3 (3)	-	-	-	-	24.8 ~ 25.3 L	25.0 (4)	-	-	-	-
		Cluster	4 ~ 7	100	-57.4	-57.4 (1)	-	-	-	-	24.3 ~ 25.7 L	24.8 (3)	-	-	-	-
		Cluster	9 ~ 12	15	-	-	-0.8 ~ -0.8	-0.8 (2)	-	-	-	-	1.4	1.4 (1)	227.1 ~ 267.5	252.7 (3)
		Cluster	7 ~ 15	15	-	-	-0.6 ~ -0.8	-0.7 (3)	-	-	-	-	1.0 ~ 1.4	1.2 (3)	189.0 ~ 226.9	207.3 (3)
GC01-103	Quartz-1 (strongly deformed)	Random	9 ~ 12	15	-	-	-1.1 ~ -1.5	-1.3 (4)	-	-	-	-	1.9 ~ 2.6	2.1 (4)	152.6 ~ 205.8	179.1 (5)
		Random	6 ~ 12	15	-	-	-4.1	-4.1 (1)	4.1	4.1 (1)	-	-	-	-	210.5 ~ 251.0	2243. (3)
			9 ~ 9	95	-57.7	-57.7 (1)	-	-	-	-	23.3 L	23.3 L	-	-	-	-
		Random	8 ~ 8	12	-	-	-3.9 ~ -4.0	-4.0 (2)	5.4	5.4 (1)	-	-	-	-	220.5 ~ 226.2	223.4 (2)
			9 ~ 15	100	-57.2 ~ -57.5	-57.4 (2)	-	-	-	-	26.8 ~ 27.8 L	27.3 (2)	-	-	-	-
		Random	7 ~ 8	15	-	-	-3.4	-3.4 (1)	-	-	-	-	-	-	218.2 ~ 232.5	224.9 (2)
		Random	6 ~ 8	10	-	-	-1.2 ~ -1.8	-1.5 (2)	-	-	-	-	2.1 ~ 3.0	2.6 (2)	181.2 ~ 207.0	194.1 (2)
	Quartz-2	Cluster	6 ~ 10	15	-	-	-3.1	-3.1 (1)	7.6	7.6 (1)	-	-	-	-	224.8 ~ 239.9	230.0 (3)
		Isolated	10	10	-	-	-0.6	-0.6 (1)	-	-	-	-	1.0	1.0 (1)	258.4	258.4 (1)
		Cluster	6 ~ 10	20	-	-	-2.5 ~ -2.5	-2.5 (2)	-	-	-	-	4.2 ~ 4.2	4.2 (2)	233.6 ~ 280.2	256.9 (2)
	Sphalerite	Isolated	15	20	-	-	-1.6	-1.6 (1)	-	-	-	-	2.7	2.7 (1)	248.9	248.9 (1)
		Isolated	28	10	-	-	-2.3	-2.3 (1)	-	-	-	-	3.9	3.9 (1)	155.9	155.9 (1)
		Isolated	15	30	-	-	-0.1	-0.1 (1)	-	-	-	-	0.2	0.2 (1)	285.6	285.6 (1)
		Cluster	13 ~ 30	30	-	-	-0.1 ~ -0.1	-0.1 (3)	-	-	-	-	0.2 ~ 0.2	0.2 (3)	286.1 ~ 291.0	289.0 (3)
		Cluster	7 ~ 28	30	-	-	-0.1	-0.1 (1)	-	-	-	-	0.2	0.2 (1)	279.1 ~ 284.2	282.5 (3)
GC01-160	Quartz-2	Cluster	5 ~ 8	10	-	-	-0.5 ~ -0.7	-0.6 (3)	-	-	-	-	0.9 ~ 1.2	1.0 (3)	194.9 ~ 216.0	204.7 (3)
		Isolated	4	10	-	-	-0.5	-0.5 (1)	-	-	-	-	0.9	0.9 (1)	180.3	180.3 (1)
		Scattered	7 ~ 12	10	-	-	-3.7	-3.7 (1)	5.2	5.2 (1)	-	-	-	-	205.3 ~ 262.0	232.9 (3)
		Cluster	4 ~ 9	10	-	-	-3.4 ~ -4.2	-3.8 (2)	-	-	-	-	5.5 ~ 6.7	6.1 (2)	228.3 ~ 250.3	243.1 (4)
Jimmy Hill																
GC01-08	Quartz	Cluster	5 ~ 5	25	-	-	-	-	-	-	-	-	-	-	231.2 ~ 257.8	244.5 (2)
		Cluster	6 ~ 8	20	-	-	-	-	-	-	-	-	-	-	235.0 ~ 238.6	236.8 (2)
		Cluster	4 ~ 8	10	-	-	-12.9	-12.9 (1)	-	-	-	-	16.8	16.8 (1)	225.2 ~ 244.5	234.9 (2)
			10	90	-58.2	-58.2 (1)	-	-	1.0	1.0 (1)	19.2 L	19.2 (1)	14.4	14.4 (1)	285.1 V	285.1 (1)
		Cluster	7 ~ 10	15	-	-	-8.0	-8.0 (1)	-	-	-	-	11.7	11.7 (1)	306.6 ~ 319.6	311.8 (4)
		Cluster	9 ~ 12	20	-	-	-8.5	-8.5 (1)	-	-	-	-	12.3	12.3 (1)	325.5 ~ 344.5	331.7 (4)
			12	100	-60.0	-60.0 (1)	-	-	-	-	13.6 L	13.6 (1)	-	-	-	-
		Cluster	13	100	-58.6	-58.6 (1)	-	-	-	-	17.5 L	17.5 (1)	-	-	-	-
			8	15	-	-	-	-	-	-	-	-	-	-	255.6	255.6 (1)
		Cluster	12	100	-57.6	-57.6 (1)	-	-	-	-	22.6 L	22.6 (1)	-	-	-	-
			8 ~ 10	10	-	-	-	-	-	-	-	-	-	-	166.1 ~ 181.3	173.7 (2)
											Tm-halite					
		Isolated	16	20	-	-	-	-	-	-	263.2	263.2 (1)	35.7	35.7 (1)	401.1	401.1 (1)
		Isolated	13	10	-	-	-	-	-	-	258.5	258.5 (1)	35.4	35.4 (1)	239.8	239.8 (1)
Kedron																
GC01-10	Quartz	Random	12	5	-	-	-	-	-	-	263.5	263.5 (1)	35.7	35.7 (1)	122.6	122.6 (1)
		Random	8	5	-	-	-	-	-	-	175.2	175.2 (1)	30.9	30.9 (1)	153.2	153.2 (1)
		Random	8 ~ 13	5	-	-	-	-	-	-	145.6 ~ 204.8	165.4 (4)	29.7 ~ 32.2	30.5 (4)	127.4 ~ 162.0	137.5 (4)
		Random	7 ~ 10	5	-	-	-	-	-	-	127.9 ~ 167.0	147.5 (2)	29.0 ~ 30.5	29.8 (2)	134.0 ~ 162.7	151.1 (3)
		Cluster	4 ~ 7	8	-	-	-10.3 ~ -14.8	-12.6 (2)	-	-	-	-	14.3 ~ 18.5	16.4 (2)	186.1 ~ 207.4	196.9 (4)
		Random	6 ~ 9	8	-	-	-	-	-	-	152.7	152.7 (1)	29.9	29.9 (1)	181.5 ~ 191.4	185.9 (3)

$T_{m\text{-}clath}$ = melting temperature of clathrate
$T_{m\text{-}ice}$ = ice melting temperature
$T_{m\text{-}CO_2}$ = melting temperature of CO_2

$T_{h\text{-}CO_2}$ = homogenization temperature of CO_2
Th = homogenization temperature
V/T = vapour/total ratio

2.4 to 7.8 weight per cent NaCl equivalent. No CO_2 was detected in some liquid-rich inclusions, because it was either absent or too low to be detected by microthermometry.

Vapour-rich fluid inclusions show melting temperatures of CO_2 from -57.3°C to -57.1°C and homogenization temperatures of CO_2 from +17.5°C to +25.9°C (to liquid) (Table 1; Fig. 3).

Fluid pressures estimated from isochores of the vapour-rich inclusions, with temperatures approximated by those of liquid-rich inclusions (220°–280°C), range from 785 to 1364 bars (shaded area in Fig. 3e). These pressures correspond to lithostatic depths of 2.9 to 5.1 km.

Clarence Stream

Four samples from Clarence Stream were selected for fluid-inclusion study. Two (GC01-141, GC01-150) are from a pegmatite vein and two (GC01-103, GC01-160) are from quartz veins. Gold concentrations are 0.007 ppm (GC01-150), 0.17 ppm (GC01-103), and >5.0 ppm (GC01-160). Note samples GC01-141 and GC01-150 are from the same pegmatite vein that ran 9.11 ppm Au (Thorne et al., 2001). Both pegmatite and quartz veins were subject to postmineralization deformation (Fig. 4a, d). Quartz in the pegmatite vein shows slight undulatory extinction under crossed nicols (Fig. 4b). Two types of quartz are distinguished in the deformed quartz veins, i.e. quartz inundated by fluid inclusions and showing strong undulatory extinction, and quartz having relatively few fluid inclusions and showing moderate to weak undulatory extinction (Quartz-2; Fig. 4e, f). Quartz-2 probably resulted from the recrystalization of quartz-1. Sample GC01-103 contains significant amounts of sphalerite that appears to be associated with quartz-2.

As for Poplar Mountain, three types of fluid inclusions were found: liquid-rich (vapour/total ratio ≤30%), vapour-rich (vapour/total ratio near 100%, i.e. liquid phase invisible), and those with varied vapour/total ratios (Fig. 4c, g). Unlike Poplar Mountain, however, CO_2 is either very low or absent in liquid-rich inclusions. The presence of CO_2 in these liquid-rich inclusions is manifested only by the formation of clathrates. Table 1 provides microthermometry results for individual fluid-inclusion assemblages.

Pegmatite quartz

Vapour-rich fluid inclusions from pegmatite quartz show melting temperatures of CO_2 from -58.7°C to -57.3°C (Fig. 5a), suggesting the presence of other gases (e.g. CH_4) in addition to CO_2. Homogenization temperatures of CO_2 range from +20.8°C to +25.0°C (to liquid), with an exception at 16.6°C (to vapour) (Fig. 5b). Liquid-rich fluid inclusions show ice melting temperatures from -11.4°C to -0.2°C, gas hydrate melting temperatures from +7.0°C to +29.7°C (Table 1), and final homogenization temperatures mainly from 180°C to 280°C (Fig. 5c). The high melting temperatures of gas hydrates suggest the probable presence of H_2S. For fluid inclusions that do not contain detectable gas hydrates, fluid salinities calculated from ice melting temperatures range from 0.4 to 13.9 weight per cent NaCl equivalent.

Quartz-1

Vapour-rich fluid inclusions from quartz-1 show melting temperatures of CO_2 from -57.7°C to -57.4°C (Fig. 5a) and homogenization temperatures of CO_2 from +23.3°C to +27.3°C (to liquid) (Fig. 5b). Liquid-rich fluid inclusions show ice-melting temperatures from -4.0°C to -1.3°C, gas hydrate melting temperatures from +4.1°C to +5.4°C (Table 1), and final homogenization temperatures mainly from 180°C to 225°C (Fig. 5c). For fluid inclusions that do not contain detectable gas hydrates, fluid salinities calculated from ice melting temperatures range from 2.1 to 2.6 weight per cent NaCl equivalent.

Quartz-2 and sphalerite

Liquid-rich fluid inclusions in quartz-2 and sphalerite (Fig. 4h) show ice melting temperatures from -3.8°C to -0.1°C, gas hydrate melting temperatures from +5.2°C to +7.6°C, and final homogenization temperatures mainly from 180°C to 280°C. Salinities range from 0.2 to 6.1 weight per cent NaCl equivalent.

Fluid pressures estimated from isochores of the vapour-rich inclusions from pegmatite quartz (except the one homogenized to vapour) and quartz-1 in quartz veins, with temperatures approximated by those of liquid-rich inclusions (180°–280°C), range from 594 to 1226 bars (shaded area in Fig. 5d), corresponding to lithostatic depths of 2.2 to 4.5 km.

Jimmy Hill

One sample from a major quartz vein (GC01-08) was selected for fluid-inclusion study. Its gold concentration is >5.0 ppm. Liquid-rich, vapour-rich, and heterogeneously trapped fluid inclusions are abundant. Liquid-rich fluid inclusions show

Figure 4. *Petrography of fluid inclusions and host minerals from the Clarence Stream gold occurrence.* ***a****) A pegmatite vein (trench 4);* ***b****) quartz from the pegmatite vein, showing slight undulatory extinction under crossed nicols (GC01-150);* ***c****) coexistence of vapour-rich and liquid-rich fluid inclusions in pegmatite quartz (GC01-150);* ***d****) a boudinaged quartz vein (trench 7);* ***e, f****) two generations of quartz: residual quartz (quartz-1) is inundated by fluid inclusions (e) and shows strong undulatory extinction and subgrains under crossed nicols (f), whereas recrystallized quartz (quartz-2) is relatively free of fluid inclusions and shows uniform extinction (GC01-160);* ***g****) coexistence of vapour-rich, liquid-rich, and heterogeneously trapped fluid inclusions in quartz-1 (GC01-160);* ***h****) liquid-rich fluid inclusions in sphalerite; note consistent vapour/total ratios.*

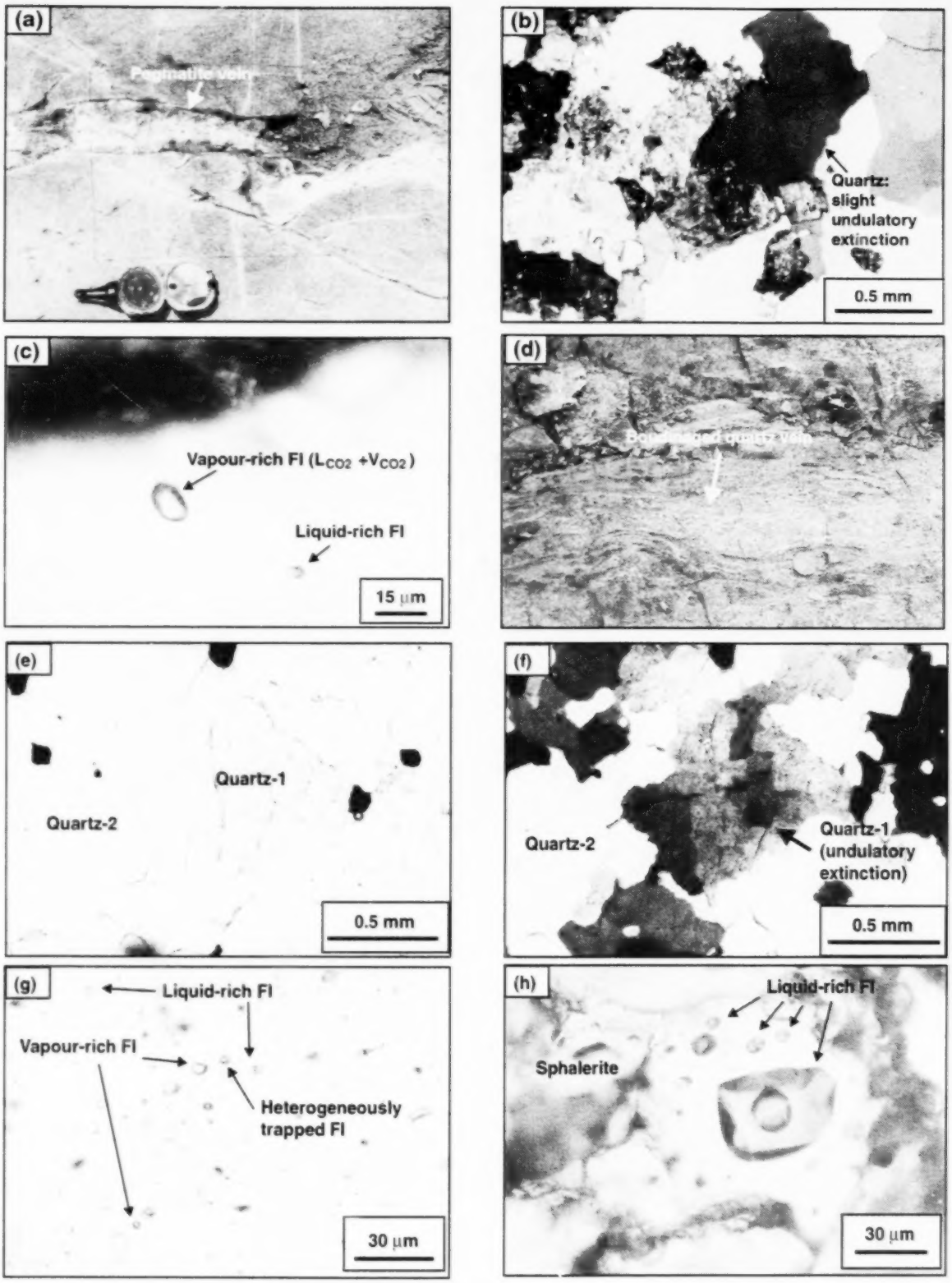
(a)
(b)
Quartz: slight undulatory extinction
0.5 mm
(c)
Vapour-rich FI (L_{CO2} +V_{CO2})
Liquid-rich FI
15 μm
(d)
(e)
Quartz-1
Quartz-2
0.5 mm
(f)
Quartz-2
Quartz-1 (undulatory extinction)
0.5 mm
(g)
Liquid-rich FI
Vapour-rich FI
Heterogeneously trapped FI
30 μm
(h)
Liquid-rich FI
Sphalerite
30 μm

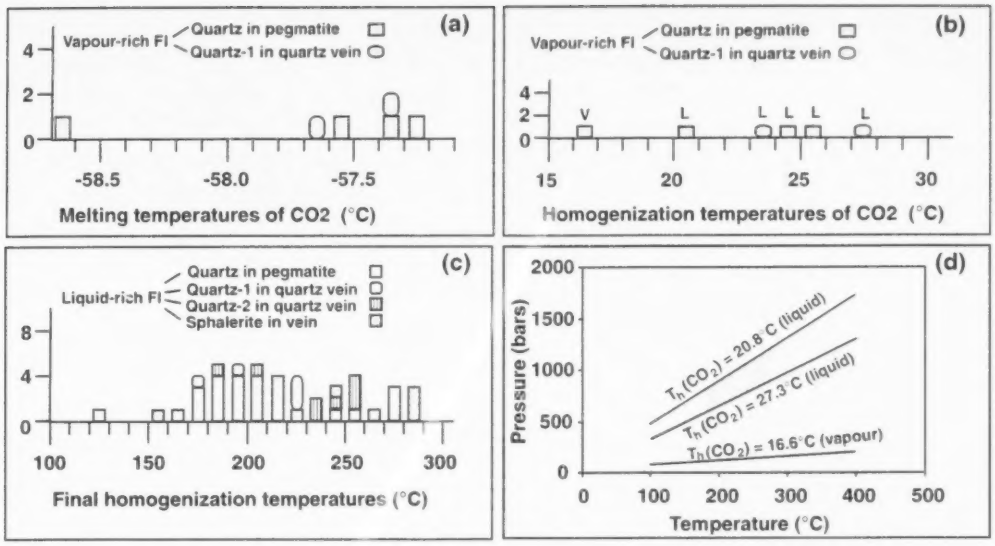

Figure 5. *Microthermometry data for fluid inclusions from the Clarence Stream gold occurrence.* ***a****) Histogram of melting temperatures of* CO_2*;* ***b****) histogram of homogenization temperatures of* CO_2*;* ***c****) histogram of final homogenization temperatures;* ***d****) isochores of vapour-rich fluid inclusions (approximated by* CO_2*), showing possible range of fluid temperature and pressure (shaded area).*

ice melting temperatures from -12.9°C to -8.0°C, corresponding to salinities of 16.8 to 11.7 weight per cent NaCl equivalent, and homogenization temperatures from 174°C to 401°C (Table 1). Some liquid-rich inclusions contain a halite crystal that melts at temperatures from 258.5°C to 263.2°C, corresponding to salinities of 35.4 to 35.7 weight per cent NaCl equivalent. Vapour-rich fluid inclusions show melting temperatures of CO_2 from -60.0°C to -57.6°C and homogenization temperatures of CO_2 from 13.6°C to 22.6°C (to liquid) (Table 1). Fluid pressures estimated from the isochores of vapour-rich inclusions, with temperatures approximated by those of liquid-rich inclusions (mainly 230°–330°C), range from 965 to 1764 bars, corresponding to lithostatic depths of 3.6 to 6.5 km.

Kedron

One sample (GC01-10) was studied for fluid inclusions. Its gold concentration is 0.017 ppm. Three types of fluid inclusions are found: liquid-rich, vapour-rich, and heterogeneously trapped. Unlike those from the other gold occurrences, the vapour-rich fluid inclusions from Kedron do not contain detectable CO_2. Liquid-rich fluid inclusions include those with liquid+vapour and those with liquid+vapour+halite. Halite dissolution temperatures range from 147.5°C to 263.5°C, corresponding to salinities from 29.8 to 35.7 weight per cent NaCl equivalent. Homogenization temperatures (bubble disappearance) range from 122.6°C to 196.9°C.

DISCUSSION AND CONCLUSIONS

The gold occurrences that are spatially associated with granite intrusions in southwestern New Brunswick share some similarities with a newly recognized type of intrusion-related gold systems (Thompson et al., 1999; Lang et al., 2000; Lang and Baker, 2001), including tectonic setting, granite geochemistry, mineralization styles, and ore geochemistry (Chi et al., 2002; McLeod, 2002). This paper has added new information about their similar fluid compositions.

The fluid-inclusion microthermometry data presented here suggest that the mineralizing fluid systems for three gold occurrences (Poplar Mountain, Clarence Stream, and Jimmy Hill) may be approximated by the H_2O-NaCl-CO_2-CH_4 system, which is characteristic, although not diagnostic, of the deeper part of the newly recognized type of intrusion-related gold systems (Lang et al., 2000). A similar fluid composition system has been documented for the Lake George W-Mo-Au-Sb deposit (Seal et al., 1987). The fluid inclusions from Kedron may be approximated by H_2O-NaCl with high salinities, which is characteristic of the shallower part of the newly recognized type of intrusion-related gold systems and the porphyry base metal-gold systems (Lang et al., 2000). The fluid-inclusion data suggest the coexistence of liquid and vapour during mineralization at each of the gold occurrences, but it cannot be determined whether this was caused by fluid-phase separation at the site of mineralization or by two-phase flow.

The Poplar Mountain gold occurrence is hosted by volcanic and subvolcanic rocks and shows alteration characteristics that may be compared to epithermal systems or the outer part of porphyry systems (Chi and Watters, 2002). However, the high fluid pressures estimated from fluid inclusions (785–1364 bars) and the corresponding lithostatic depths (2.9–5.1 km) suggest that gold mineralization probably took place after significant burial of the host rocks. The mineralization event may be related to deep-seated magmatic intrusions or to the regional-scale Woodstock Fault. The variation of fluid pressures may be related to the fluctuation of pressure systems, e.g. between hydrostatic and lithostatic loads.

In the case of the Clarence Stream occurrence, the relatively low fluid pressures (594–1226 bars) and corresponding lithostatic depths (2.2–4.5 km), compared to the depth of emplacement of the Magaguadavic granite (about 2 km), suggest that gold mineralization probably took place after some erosion of the overburden following granite emplacement. As is the case for the Poplar Mountain occurrence, the variation of fluid pressures may be related to the fluctuation of pressure systems. However, considering the postmineralization deformation and the limited number of fluid inclusions studied, the author as yet cannot rule out the possibility that fluid inclusions in pegmatite quartz and in the residual quartz (quartz-1) in the quartz veins were modified by deformation of the host mineral. Furthermore, the relatively low homogenization temperatures of fluid inclusions from the quartz in the pegmatite suggest that the quartz has likely been recrystallized.

In conclusion, this study shows that gold occurrences that are spatially associated with granite intrusions in southwestern New Brunswick formed from fluid systems similar to those of the newly recognized type of intrusion-related gold systems. However, the microthermometry study of fluid inclusions is only the first step toward understanding the fluid composition and temperature and pressure conditions. Microanalyses of fluid inclusions (e.g. laser-raman and laser-ICP-MS) are warranted for a better understanding of the fluid systems.

ACKNOWLEDGMENTS

This study is financially supported by the Geological Survey of Canada Targeted Geoscience Initiative (TGI) Program, in collaboration with the New Brunswick Department of Natural Resources and Energy, the University of New Brunswick, and Freewest Resources Canada Inc. I would like to thank Sheila Watters, Xueming Yang, and Kay Thorne for assistance with field work, and Malcolm McLeod, Les Fyffe, David Lentz, Don Hoy, and Benoît Dubé for discussions on regional geology and metallogeny. The critical review by Dan Kontak improved the quality of this paper.

REFERENCES

Brown, P.E.
1989: FLINCOR: a microcomputer program for the reduction and investigation of fluid inclusion data: American Mineralogy, v. 74, p. 1390–1393.

Chi, G. and Watters, S.
2002: Preliminary geological and petrographic study of the Poplar Mountain Au occurrence, southwestern New Brunswick: Geological Survey of Canada, Current Research 2002-D6, 11 p.

Chi, G., Davis, W., Watters, S., Fyffe, L.R., McLeod, M.J., Lentz, D.R., Yang, X., Thorne, K., Castonguay, S., Tremblay, A., Dubé, B., Savard, M.M., Johnson, S., Lauzière, K., Rennick, P., and Hoy, D.
2002: Metallogeny of intrusion-related gold systems in southwestern New Brunswick: Prospectors and Developers Association of Canada, International Convention, Trade Show, and Investors Exchange 2002 (Toronto), poster.

Fyffe, L.R., Pickerill, R.K., and Stringer, P.
1999: Stratigraphy, sedimentology and structure of the Oak Bay and Waweig formations, Mascarene Basin: implications for the paleotectonic evolution of southwestern New Brunswick: Atlantic Geology, v. 35, p. 59–84.

Lang, J.R. and Baker, T.
2001: Intrusion-related gold systems: the present level of understanding: Mineralium Deposita, v. 36, p. 477–489.

Lang, J.R., Baker, T., Hart, C.J., and Mortensen, J.K.
2000: An exploration model for intrusion related gold systems: SEG Newsletter, No. 40, p. 1–15.

McLeod, M.J.
2002: An emerging gold district in southern New Brunswick: tectonic setting, models and future prospects: Prospectors and Developers Association of Canada, International Convention, Trade Show, and Investors Exchange 2002 (Toronto), Technical Program and Core Shack Abstracts, p. 15.

McLeod, M.J. and McCutcheon, S.R.
2000: Gold environments in New Brunswick: New Brunswick Department of Natural Resources and Energy, Minerals and Energy Division, Plate 2000-8.

McLeod, M.J., Johnson, S.C., and Ruitenberg, A.A.
1994: Geological map of the southwestern New Brunswick (1:250 000): New Brunswick Department of Natural Resources and Energy, Mineral Resources, Map NR-5.

Morrissy, C.J.
1991: Gold assessment at the Lake George mine, York County, New Brunswick: New Brunswick Department of Natural Resources and Energy, Mineral Resources, Open File Report 91-1, 22 p.

New Brunswick Department of Natural Resources and Energy
2000: Bedrock geology of New Brunswick, Map NR-1 (2000 edition), scale: 1:500 000.

Robertson, R.
2001: NB gold project generates interest: The Northern Miner, V. 87, no. 20, p. 1–2.

Seal, R.R., II, Clark, A.H., and Morrissy, C.J.
1987: Stockwork tungsten (scheelite)-molybdenum mineralization, Lake George, southwestern New Brunswick: Economic Geology, v. 82, p. 1259–1282.

Thompson, J.F.H., Sillitoe, R.H., Baker, T., Lang, J.R., and Mortensen, J.K.
1999: Intrusion-related gold deposits associated with tungsten-tin provinces: Mineralium Deposita, v. 34, p. 323–334.

Thorne, K.G., Hoy, D., and Lentz, D.R.
2001: Field guidebook: the Clarence Stream gold deposit, southwestern New Brunswick: New Brunswick Department of Natural Resources and Energy, Mineral and Energy Division, Open File 2001-9, 16 p.

van Staal, C.
1994: Brunswick subduction complex in the Canadian Appalachians: record of the Late Ordovician to Late Silurian collision between Laurentia and the Gander margin of Avalon: Tectonics, v. 13, p. 946–962.

Williams, H.
1995: Temporal and spatial divisions: *in* Chapter 2, Geology of the Appalachian-Caledonian Orogen in Canada and Greenland, (ed.) H. Williams; Geological Survey of Canada, Geology of Canada, no. 6, p. 21–44.

Geological Survey of Canada Project 010008